

RESEARCH PAPER

# Identification and utilization of a sow thistle powdery mildew as a poorly adapted pathogen to dissect post-invasion non-host resistance mechanisms in *Arabidopsis*

Yingqiang Wen<sup>1,2</sup>, Wenming Wang<sup>2,3</sup>, Jiayue Feng<sup>1,2</sup>, Ming-Cheng Luo<sup>4</sup>, Kenichi Tsuda<sup>5</sup>, Fumiaki Katagiri<sup>5</sup>, Gary Bauchan<sup>6</sup> and Shunyuan Xiao<sup>2,3,\*</sup>

<sup>1</sup> College of Horticulture and College of Life Sciences, Northwest A&F University, Yangling, Shaanxi, People's Republic of China

<sup>2</sup> Institute for Bioscience and Biotechnology Research, University of Maryland, Shady Grove, Maryland, USA

<sup>3</sup> Department of Plant Sciences and Landscape Architecture, University of Maryland, College Park, Maryland, USA

<sup>4</sup> Department of Plant Sciences, University of California, Davis, California, USA

<sup>5</sup> Department of Plant Biology, University of Minnesota, St Paul, Minnesota, USA

<sup>6</sup> Electron and Confocal Microscopy Unit, USDA-ARS, Beltsville, Maryland, USA

\* To whom correspondence should be addressed. E-mail: [xiao@umd.edu](mailto:xiao@umd.edu)

Received 4 October 2010; Revised 16 November 2010; Accepted 18 November 2010

## Abstract

To better dissect non-host resistance against haustorium-forming powdery mildew pathogens, a sow thistle powdery mildew isolate designated *Golovinomyces cichoracearum* UMSG1 that has largely overcome penetration resistance but is invariably stopped by post-invasion non-host resistance of *Arabidopsis thaliana* was identified. The post-invasion non-host resistance is mainly manifested as the formation of a callosic encasement of the haustorial complex (EHC) and hypersensitive response (HR), which appears to be controlled by both salicylic acid (SA)-dependent and SA-independent defence pathways, as supported by the susceptibility of the *pad4/sid2* double mutant to the pathogen. While the broad-spectrum resistance protein RPW8.2 enhances post-penetration resistance against *G. cichoracearum* UCSC1, a well-adapted powdery mildew pathogen, RPW8.2, is dispensable for post-penetration resistance against *G. cichoracearum* UMSG1, and its specific targeting to the extrahaustorial membrane is physically blocked by the EHC, resulting in HR cell death. Taken together, the present work suggests an evolutionary scenario for the *Arabidopsis*–powdery mildew interaction: EHC formation is a conserved subcellular defence evolved in plants against haustorial invasion; well-adapted powdery mildew has evolved the ability to suppress EHC formation for parasitic growth and reproduction; RPW8.2 has evolved to enhance EHC formation, thereby conferring haustorium-targeted, broad-spectrum resistance at the post-invasion stage.

**Key words:** Callose, encasement of haustorial complex, extrahaustorial membrane, haustorium, jasmonic acid, non-host resistance, post-invasion resistance, powdery mildew, RPW8, salicylic acid.

## Introduction

Plants have evolved a multilayered immune system to prevent colonization by most potential pathogens. For non-adapted pathogens, plants exhibit non-host resistance, which is operative and effective in all individuals in a given plant species/genus (Hadwiger and Culley, 1993; Thordal-Christensen, 2003). Non-host resistance in most cases is a manifestation of the innate immune response triggered

upon recognition of pathogen-associated molecular patterns (PAMPs) (Chisholm *et al.*, 2006). A successful pathogen, by definition, must have conquered this basal immune system and be able to establish colonization on the defeated plant (then a host). Conceivably, the host plant does not simply yield; rather it still actively fights against the pathogen to limit the severity of the infection. This is achieved through

a defence layer(s) operative in susceptible hosts that is often referred to as basal resistance (Dangl and Jones, 2001). However, for a well-adapted pathogen race, basal resistance is not sufficient to stop the invasive growth and reproduction of the pathogen. In response, the host utilizes a new branch of the immune system controlled by resistance (*R*) genes often encoding intracellular immune receptors of the nucleotide-binding site and leucine-rich-repeat (NB-LRR) superfamily to trigger stronger and race-specific resistance (Chisholm *et al.*, 2006; Jones and Dangl, 2006). Atypical *R* genes encoding proteins distinct from NB-LRRs have also been identified. For example, *RPW8* from *Arabidopsis* confers broad-spectrum resistance against well-adapted powdery mildew pathogens (Xiao *et al.*, 2001). Interestingly, basal resistance, *RPW8*-mediated resistance, and race-specific resistance triggered by a subset of NB-LRR *R* proteins containing an N-terminal Toll/interleukin-1 receptor (TIR) homology domain share some common essential signalling components such as EDS1 and PAD4 (Aarts *et al.*, 1998; Reuber *et al.*, 1998; Falk *et al.*, 1999; Jirage *et al.*, 1999; Xiao *et al.*, 2003). In addition, the *Arabidopsis eds1* mutant plants and plants expressing *NahG*, the gene encoding a bacterial enzyme that converts salicylic acid (SA) to catechol, were also reported to be compromised in non-host resistance (Parker *et al.*, 1996; Mellersh and Heath, 2003; Zimmerli *et al.*, 2004). Thus, non-host resistance and host resistance may be evolutionarily interrelated and mechanistically interconnected (Nurnberger *et al.*, 2004). However, how these resistance forms are interconnected remains unclear mainly because non-host resistance as a whole is still poorly understood.

Non-host resistance against a biotrophic fungal pathogen is often manifested as the ability of the attacked plant to prevent fungal penetration (thus named penetration resistance), or the ability to terminate the development and/or functioning of the fungal feeding structure such as the intracellular hypha or the haustorium before it extracts enough nutrition from the plant cells for reproduction (thus referred to as post-invasion resistance) (Thordal-Christensen, 2003). Genetic studies of penetration (PEN) resistance using barley powdery mildew (*Blumeria graminis* f.sp. *hordei*; *Bgh*), as a non-adapted pathogen of *Arabidopsis*, have revealed at least two separate pathways contributing to penetration resistance. One involves an exocytosis pathway controlled by the PEN1 syntaxin and its working partners (Collins *et al.*, 2003; Kwon *et al.*, 2008) and the other requires the PEN2 myrosinase and the PEN3 ATP-binding cassette transporter (Lipka *et al.*, 2005; Stein *et al.*, 2006; Bednarek *et al.*, 2009; Clay *et al.*, 2009). Impairing either or both of the two pathways does not seem to break down the post-invasion resistance, as there is no colonization of barley powdery mildew *Bgh* and pea powdery mildew (*Erysiphe pisi*) on *pen1* and *pen2* single or *pen1 pen2* double mutants (Lipka *et al.*, 2005). However, further loss of EDS1 or PAD4/SAG101 in the *pen2* or *pen3* mutant background results in breakdown of the post-invasion resistance of *Arabidopsis* to permit microcolonization of *Bgh* and macrocolonization of *E. pisi* (Lipka *et al.*, 2005; Stein *et al.*, 2006).

These findings suggest that for a non-adapted powdery mildew to adapt a given plant species it has sequentially to overcome multilayered defence barriers of the attacked plant. These findings also imply that for a given plant species there are probably non-host powdery mildews in the natural ecosystem that have conquered penetration resistance but are stopped by post-invasion resistance. Here, the identification of such a powdery mildew isolate relative to *Arabidopsis* that can largely overcome penetration resistance, but its further haustorium development and function is arrested by post-invasion resistance, is reported. This isolate was thus used as a tool to dissect the genetic mechanisms involved in post-invasion resistance using the *Arabidopsis* model system.

## Materials and methods

### Plant lines and growth conditions

Twenty-five *Arabidopsis thaliana* accessions (Bg-1, Bu-11, Bu-23, C24, Can-0, Col-0, Do-0, Es-0, FL-1, FM3, Gre-0, Hs-1, Kas-1, Knox-1, Ler, Lin, Ms-0, Ob-0, Per-1, Pna10, Sg-1, Sapporo-0, Shadhara, Ta-0, and Wa-1), 13 single mutant lines (*eds1-2*, *pad4-1*, *sid2-1*, *eds5-1*, *ndr1*, *npr1-1*, *rar1-10*, *sgt1b-1*, *coil-1*, *dde2-2*, *ein2-1*, *edr2*, and *pen1-1*; all are in the Col-0 background except *eds1-2* which is in the Ler background), two double mutant line (*pad4-1/sid2-1* and *dde2-2/ein2-2*), one quadruple mutant (*dde2/ein2/pad4/sid2*), and three transgenic lines [Col-0/*NahG*, Col-0/*RPW8.2-YFP* (R2Y4), and Col-0/*RPW8.1+RPW8.2* (S5)] were used for tests with the sow thistle (*Sonchus oleraceus*) powdery mildew. The DNA construct *RPW8.2-YFP* (yellow fluorescent protein) driven by the *RPW8.2* promoter (Wang *et al.*, 2009) was introduced into *eds1-2* and *pad4-1/sid2-1* via *Agrobacterium*-mediated transformation. Seeds were sown in Sunshine Mix #1 (Maryland Plant and Suppliers, Baltimore, MD, USA) and cold treated (4 °C for 2 d), and seedlings were kept under 22 °C, 75% relative humidity, short-day (8 h light at 125  $\mu\text{mol m}^{-2} \text{s}^{-1}$ , 16 h dark) conditions for 5–6 weeks before pathogen inoculation.

### Isolation and characterization of the sow thistle powdery mildew isolate *Golovinomyces cichoracearum* (Gc) UMSG1

The sow thistle powdery mildew was identified in sow thistle (*S. oleraceus*) plants in the grassland of the University of Maryland Shady Grove campus in the summer of 2007. The fungal isolate was purified by single-colony inoculation of clean sow thistle plants for five consecutive generations. The isolate was then maintained on sow thistle plants at 22 °C (16 h light, 8 h dark) in a separate growth chamber. Genomic DNA extraction was extracted from fungal spores, and the internal transcribed spacer (ITS) rDNA fragment was amplified using the fungal genomic DNA as template and primers ITS4n, 5'-CACCTCCTCCGCT-TATTGATATGC-3' and NS7, 5'-GAGGCAATAACAGGTCTGTGATGC-3' described in Adam *et al.* (1999). The PCR product was cloned into pENTR™/D-TOPO (Invitrogen), and sequenced using plasmid DNA prepared from three positive colonies. The ITS rDNA sequence has been deposited in GenBank (accession no. HM449077). Sequence alignment between ITS rDNA sequences from different powdery mildews was performed using the AlignX function of the Vector NTI Suite (Invitrogen) and manually corrected. Phylogenetic analysis was conducted using MEGA version 4.1 (Tamura *et al.*, 2007).

### Pathogen infection and microscopy analyses

Gc UCSC1 was maintained on live *Arabidopsis* mutant *eds1-2* or *pad4-1* plants for generation of fresh inoculum. *Bgh* isolate 5874

was propagated on *Hordeum vulgare* cv. Manchuria (Haltermann *et al.*, 2001). Inoculation and visual scoring of disease reaction phenotypes were done as previously described (Xiao *et al.*, 2005). Fungal structures and dead cells in inoculated leaves were visualized with trypan blue staining (Xiao *et al.*, 2003). Callose deposited at fungal penetration sites was detected using aniline blue (0.01% in an aqueous solution containing 150 mM  $\text{KH}_2\text{PO}_4$ , pH 9.5) or sirofluor (0.1 mg ml<sup>-1</sup>; Biosupplies, <http://www.biosupplies.com.au/products.htm>) (Meyer *et al.*, 2009). *In situ* detection of  $\text{H}_2\text{O}_2$  was performed as previously described (Xiao *et al.*, 2003). At least 100 penetration sites per genotype were scored at 24 h post-inoculation (hpi) in each of the three inoculation experiments. Student's *t*-test was performed to test statistical significance for fungal penetration rate, hyphal length, and number of conidiophores per colony.  $\chi^2$  test is used to test statistical significance for two categorical variables—that is, cells with an unencased haustorium (i.e. no encasement develops around the haustorium) versus cells with an encased haustorium or undergoing the hypersensitive response (HR)—between Col-0 wild-type and any other genotypes (<http://www.ats.ucla.edu/stat/spss/whatstat/whatstat.htm>). Single or multiple channel epifluorescent images were acquired with a Zeiss Axio microscope coupled with an HBO 100 microscope illumination system. Confocal laser scanning microscopy images were acquired and processed as previously described (Wang *et al.*, 2009).

#### Scanning electron microscopy (SEM)

*Gc* UMSG1-infected sow thistle leaves, *Arabidopsis* (*eds1-2*) leaves, and *Gc* UCSC1-infected *Arabidopsis* (Col-0) leaves were used for SEM. The infected leaves were cut into 5×5 mm pieces and mounted onto flat specimen holders consisting of 16×30 mm copper plates that contained a thin layer of Tissue Tek (OCT Compound, Ted Pella, Inc., Redding, CA, USA), which acted as the cryoadhesive upon freezing. The samples were frozen conductively, in a styrofoam box, by placing the plates on the surface of a pre-cooled (−96 °C) brass bar whose lower half was submerged in liquid nitrogen ( $\text{LN}_2$ ). After 20–30 s, the holders containing the frozen samples were transferred to an  $\text{LN}_2$  Dewar for future use or cryotransferred under vacuum to the cold stage in the pre-chamber of the cryotransfer system (Polaron 2000, Quorum Technologies Ltd, East Sussex, UK). Removal of any surface contamination (condensed water vapour) took place in the cryotransfer system by etching the frozen specimens for 10–15 min by raising the temperature of the stage to −90 °C. Following etching, the temperature was lowered below −130 °C, and a magnetron sputter head equipped with a platinum target was used to coat the specimens with a very fine layer of platinum. The specimens were transferred to a pre-cooled (−140 °C) cryostage in the microscope (S4700, Hitachi High Technologies, Pleasanton, CA, USA) for observation. An accelerating voltage of 5 kV was used to observe the specimens. Images were sized and placed together to produce a single figure using Adobe® Photoshop 7.0.

## Results

### Identification and characterization of a new powdery mildew isolate infectious on sow thistles

To identify a powdery mildew isolate with limited adaptation to *Arabidopsis* for studying post-invasion resistance, powdery mildews were collected from cucumbers, tomatoes, apples, roses, and sow thistles, and *Arabidopsis* accession Col-0 grown in designated growth chambers were inoculated. Several powdery mildew collections from cucumbers and tomatoes were found to cause macrocolonization

visible to the naked eye, indicating that these pathogens are probably adapted to *Arabidopsis* and thus were discarded. Germinated conidia from several other collections, such as those from apples and roses, rarely penetrated the cell wall of Col-0 leaves, similar to those of *Bgh*, indicating that they are non-adapted mildews and their attempted invasion is stopped by penetration resistance. Interestingly, it was found that conidia of two independent collections from common sow thistle were able to penetrate Col-0 at rather high rates (~60%, see later text), suggesting that they may have gained limited adaptation to *Arabidopsis*. Thus further study focused on one of these two collections and this isolate was purified on sow thistle by five consecutive inoculations from single colonies.

The purified isolate is well adapted to the common sow thistle (belonging to *S. oleraceus* as evidenced by the plant morphology, Fig. 1A) biotype from which the original conidia were collected and to several other sow thistles with slightly different leaf morphology (data not shown). The pathogen is so aggressive on sow thistle plants that entire infected leaves could be covered by fungal mass exhibiting a typical 'powdery' look at ~12–14 days post-inoculation (dpi). To see how different this sow thistle powdery mildew is from *Gc* UCSC1, an isolate well adapted to *A. thaliana* (Adam *et al.*, 1999), the two fungi on the infected leaves of their respective hosts were first examined using SEM. The major noticeable morphological difference is the shape of the conidia. The conidia of *Gc* UCSC1 have an oval shape (20–28×14–18 µm) (Fig. 1B), with an average length-to-height ratio of  $1.53 \pm 0.14$ , whereas the conidia of the sow thistle mildew are oblong or rectangular (20–26×11–13 µm) (Fig. 1C), with an average length-to-height ratio of  $1.94 \pm 0.13$ . Also noticeable is that *Gc* UCSC1 normally has 5–6 conidia stacking on the conidiophores (Fig. 1B) whereas the sow thistle mildew has only 3–4 (Fig. 1C). Similar morphological features were observed for the sow thistle mildew on *Arabidopsis eds1-2* mutant plants which permitted fungal sporulation of this fungus (Fig. 1D).

Next, the ITS regions of rDNA of the sow thistle mildew were sequenced using primers described by Adam *et al.* (1999). Blast search showed that the full-length sequence has 98% identity to that of *Gc* UCSC1 and *G. orontii*. The 333–951 bp region of this sequence is identical to the rDNA ITS sequences of two *Gc* isolates obtained from sow thistles (*S. oleraceus* and *S. arvensis*). This sequence was then aligned with the rDNA ITS sequences from 17 different powdery mildew isolates and subjected to phylogenetic analysis using MEGA version 4 (Tamura *et al.*, 2007). The sow thistle mildew was placed in subgroup A that contains all *Gc* isolates and *G. orontii*, while *E. pisi* was in subgroup B and *Bgh* in subgroup E (Fig. 2). The sow thistle mildew isolate *Gc* UMSG1 was thus tentatively named to reflect the site of its identification (University of Maryland Shady Grove Campus).

To define *Gc* UMSG1 further, its host range, along with that of *Gc* UCSC1 and *Bgh*, was examined. *Arabidopsis* (Col-0), sow thistle (the progeny of the original sow thistle from which *Gc* UMSG1 was isolated), barley (cv. Manchuria), cucumber

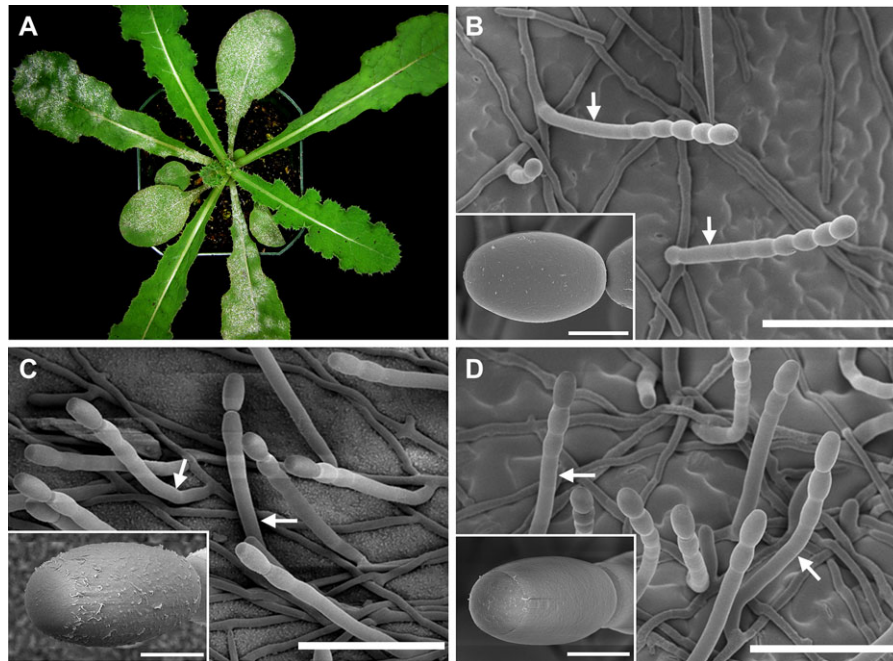


**Fig. 1.** Scanning electron micrographs illustrating morphological differences between *G. cichoracearum* UMSG1 and *G. cichoracearum* UCSC1. (A) A *Gc* UMSG1-infected sow thistle plant at 10 dpi. (B–D) Micrographs showing *Gc* UCSC1 on *Arabidopsis* (B), *Gc* UMSG1 on sow thistle (C), and *Gc* UMSG1 on *Arabidopsis eds1-2* mutant (D), respectively. Arrows indicate conidiophores bearing a chain of conidia. Insets in B–D are typical terminal conidia produced by the two fungi. Bar, 100  $\mu$ m or 10  $\mu$ m (inset).

(cv. Straight 8), tomato (cv. Moneymaker), and *Nicotiana benthamiana* were inoculated with the three isolates and the inoculated leaves were examined by trypan blue staining at 7 dpi. The fungal invasiveness was examined by looking at (i) conidium germination and hyphal growth, and (ii) fungal reproduction (sporulation). Based on the observations (Table 1), it is clear that the three isolates have distinct host ranges and *Gc* UMSG1 is only infectious (i.e. able to reproduce) on sow thistle. However, it was noted that *Gc* UMSG1 seemed to have some limited hyphal growth on *Arabidopsis*, and was invasive on cucumber and tobacco. This pattern is similar to that of *Gc* UCSC1, albeit that *Gc* UMSG1 is less invasive in cucumber compared with *Gc* UCSC1.

#### *Post-invasion resistance renders A. thaliana a non-host to Gc UMSG1*

To determine if there is genetic variation among *Arabidopsis* accessions in the resistance response to *Gc* UMSG1, 25 geographically representative natural *Arabidopsis* accessions (see Materials and methods) collected from Europe, Asia, or the USA were inoculated with *Gc* UMSG1 and the inoculated leaves were examined by trypan blue staining. It was found that all accessions permitted very limited hyphal growth as seen in Col-0, but none supported sporulation. This result indicated that *A. thaliana* is probably a non-host to *Gc* UMSG1 at the species level and that *RPW8* is dispensable for the post-invasion resistance against *Gc* UMSG1 because accessions lacking *RPW8* (Col-0) or

containing susceptible (in relation to *Gc* UCSC1) *RPW8* alleles (Bu-11, Bu-23, and FM3) (Orgil et al., 2007) were also resistant.

Next, experiments were conducted to determine if the limited hyphal growth of *Gc* UMSG1 on Col-0 correlated with a higher penetration rate in comparison with *Bgh* using a similar method described by Collins et al. (2003). As shown in Fig. 3A and C, *Bgh* rarely (<8%) penetrated the epidermal cells of Col-0 under the experimental conditions used here. In contrast, *Gc* UMSG1 supported a penetration rate of ~62%. This penetration rate, although not as high as that of the well-adapted powdery mildew *Gc* UCSC1 (93%), is nearly eight times that of *Bgh*, suggesting that *Gc* UMSG1 has evolved the ability largely to suppress the penetration resistance of Col-0. The *pen1-1* and *eds1-2* mutants were also tested with the three mildew isolates. Similar to the results reported earlier (Collins et al., 2003), it was also found that *pen1-1* mutant plants supported ~7 times higher penetration for *Bgh* compared with that of Col-0. However, the penetration rate of *Gc* UMSG1 in *pen1-1* only slightly increased from ~62% to ~71%, suggesting that PEN1-mediated penetration resistance is largely broken down by *Gc* UMSG1. Interestingly, it was also found that the *eds1-2* mutant supported a penetration rate of 43% for *Bgh*, which is ~5 times that in Col-0, suggesting that EDS1, an essential component engaged in basal and *R*-gene mediated host resistance (Aarts et al., 1998; Falk et al., 1999; Yun et al., 2003), also contributes to penetration resistance. Similar to *pen1-1*, *eds1-2* had only an ~10% increase in penetration rate for *Gc* UMSG1, suggesting a large portion

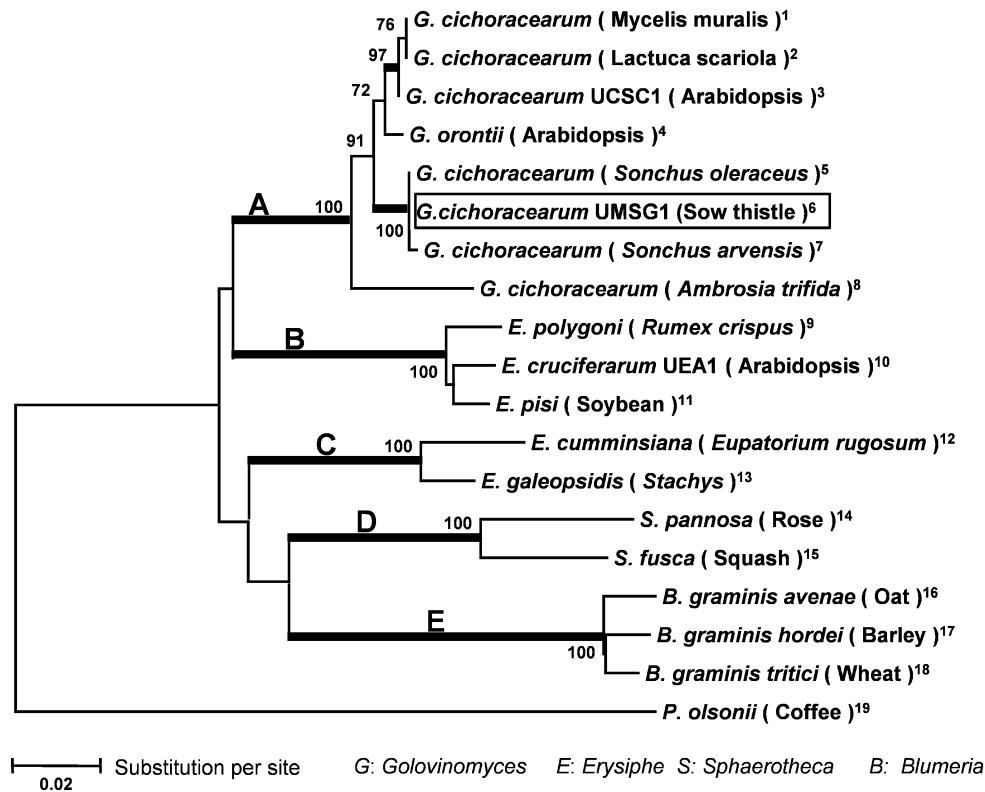


**Fig. 2.** Phylogenetic analysis of Gc UMSG1 and 17 other powdery mildew fungi based on their ITS rDNA sequences. The Neighbor-Joining tree was constructed using the alignment of the 356–951 bp region of the Gc UMSG1 with the corresponding sequences of the other 17 powdery mildew sequences by MEGA4.1 using Jukes–Cantor or p distance. The tree was rooted using the corresponding rDNA sequence of *Penicillium olsonii* as an outgroup. Bootstrap proportions of 500 bootstrap replicates >60 are indicated under the branches. Strongly supported (>95%) branches are shown in bold. Five supported clades are indicated by letters. Gc UMSG1 is boxed. GenBank accession numbers of the sequences used are as follows: 1, AB077661; 2, AB077688; 3, AF031282; 4, AF009176; 5, AY739111; 6, HM449077; 7, AB077673; 8, AF011292; 9, AF011308; 10, AF031283; 11, AF011306; 12, AF011299; 13, AF011300; 14, AF011322; 15, AF011321; 16, AF011284; 17, AF011285; 18, AF011287; 19, EF634440.

**Table 1.** Tests for the host range of *Golovinomyces cichoracearum* UMSG1

Plants of the indicated species were inoculated with one of the three powdery mildew isolates and maintained in separate growth chambers at 18–24 °C under long-day (16 h light) conditions. Inoculated leaves were collected at 3, 5, and 7 dpi and subject to trypan blue staining followed by microscopy. The amount of fungal hyphal growth and sporulation was estimated using four scales from 0 (not or rarely visible), 1 (little), 2 (some), to 3 (profuse) based on assessment of at least 200 conidia or 20 fungal colonies on leaf surfaces of each plant species at each of the three time points by trypan blue staining followed by microscopy.

Plant species	Hyphal growth			Sporulation		
	Gc UCSC1	Gc UMSG1	Bgh	Gc UCSC1	Gc UMSG1	Bgh
<i>Arabidopsis thaliana</i> (Col-0)	3	1	0	3	0	0
<i>Sonchus oleraceus</i> (sow thistle)	0	3	0	0	3	0
<i>Hordeum vulgare</i> (barley; cv. Manchuria)	0	0	3	0	0	3
<i>Cucumis sativus</i> L. (cucumber; cv. Straight 8)	3	1	0	2–3	0	0
<i>Solanum lycopersicum</i> (tomato; cv. Moneymaker)	0–1	0	0	0	0	0
<i>Nicotiana benthamiana</i> (tobacco)	1	0–1	0	0	0	0

of EDS1-mediated penetration resistance is also suppressed by Gc UMSG1. As expected, the well-adapted Gc UCSC1 completely overcame both PEN1- and EDS1-mediated resistance because *pen1-1* and *eds1-2* supported the same penetration rate as Col-0 for Gc UCSC1 (Fig. 3A, C). Interestingly, while Gc UMSG1 failed to colonize on Col-0

(Fig. 4B) or *pen1-1* (not shown) as conidiophore formation was never observed, it could successfully complete its life cycle on *eds1-2* (Fig. 1D) or Col/*NahG* plants (not shown), albeit with only a low level of sporulation.

Together, the present observations suggested that Gc UMSG1 has largely overcome penetration resistance of

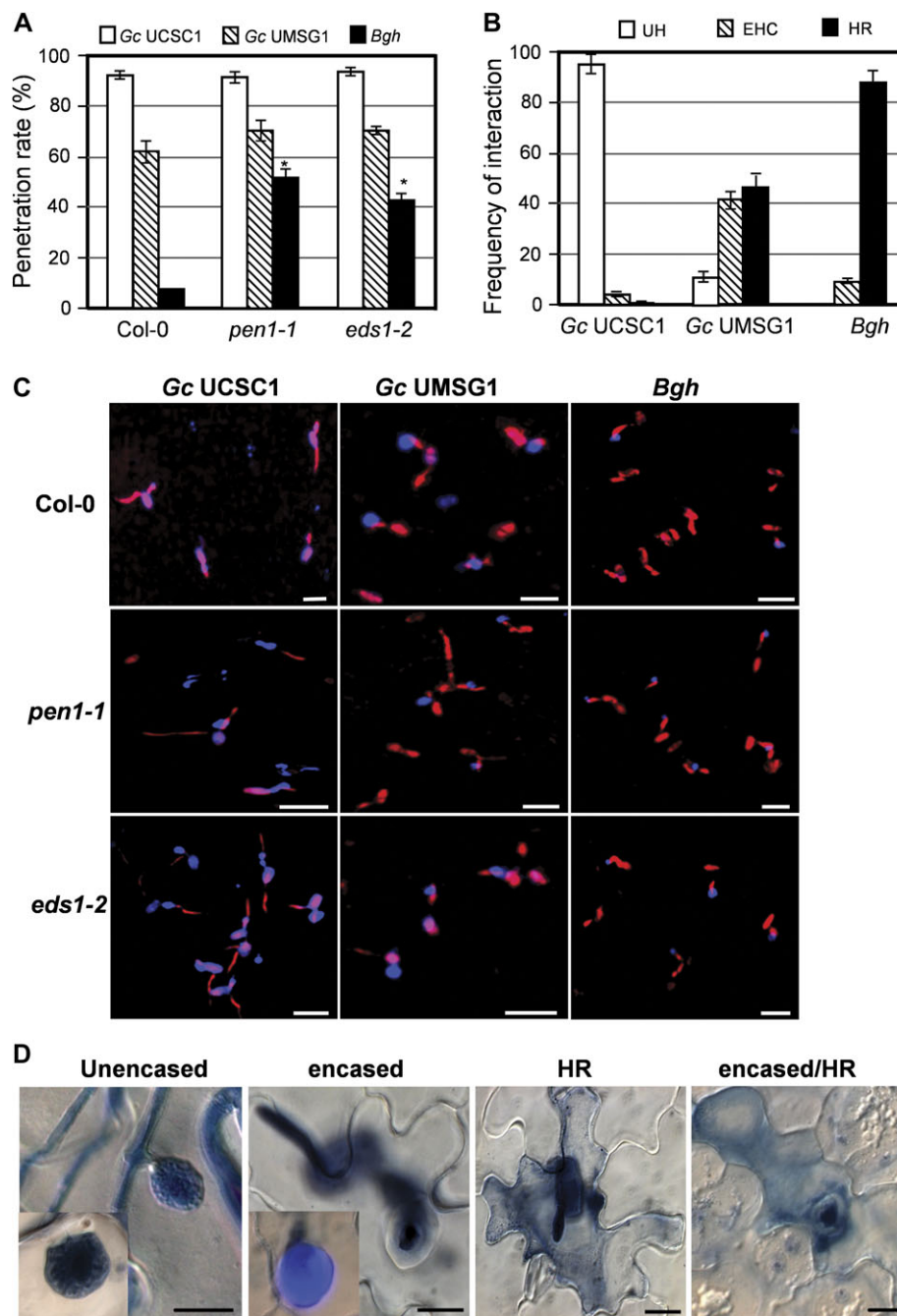


**Fig. 3.** Gc UMSG1 largely overcomes penetration resistance, but is stopped by post-invasion resistance in *Arabidopsis*. (A) Frequencies of fungal entries in leaf epidermal cells of the indicated genotypes at 24 hpi. Formation of secondary hyphae and/or haustoria was used to score for successful penetration. Data are mean  $\pm$  SEM (\* $P$  < 0.01,  $n$  = 3, Student's  $t$ -test), collected from three independent experiments (for each of which >200 interaction sites/genotype were evaluated). (B) Types and frequencies of post-invasion interaction in the leaf epidermal cells of Col-0 infected with three powdery mildew isolates. UH, cells containing an unencased (presumably healthy) haustorium (i.e. without an EHC); EHC, cells containing a haustorium with an EHC; HR, cells undergoing cell death. Data are mean  $\pm$  SEM, collected from three independent experiments (for each of which >200 interaction sites were evaluated for each isolate). (C) Representative images showing fungal penetration and hyphal growth in the three indicated genotypes at 24 hpi. Conidia and hyphae were stained red by propidium iodide, and callose deposited in papillae and/or EHC was stained blue by aniline blue. Bars, 50  $\mu$ m. (D) Representative images of three types of post-invasion interaction described in (B). Bars, 20  $\mu$ m.

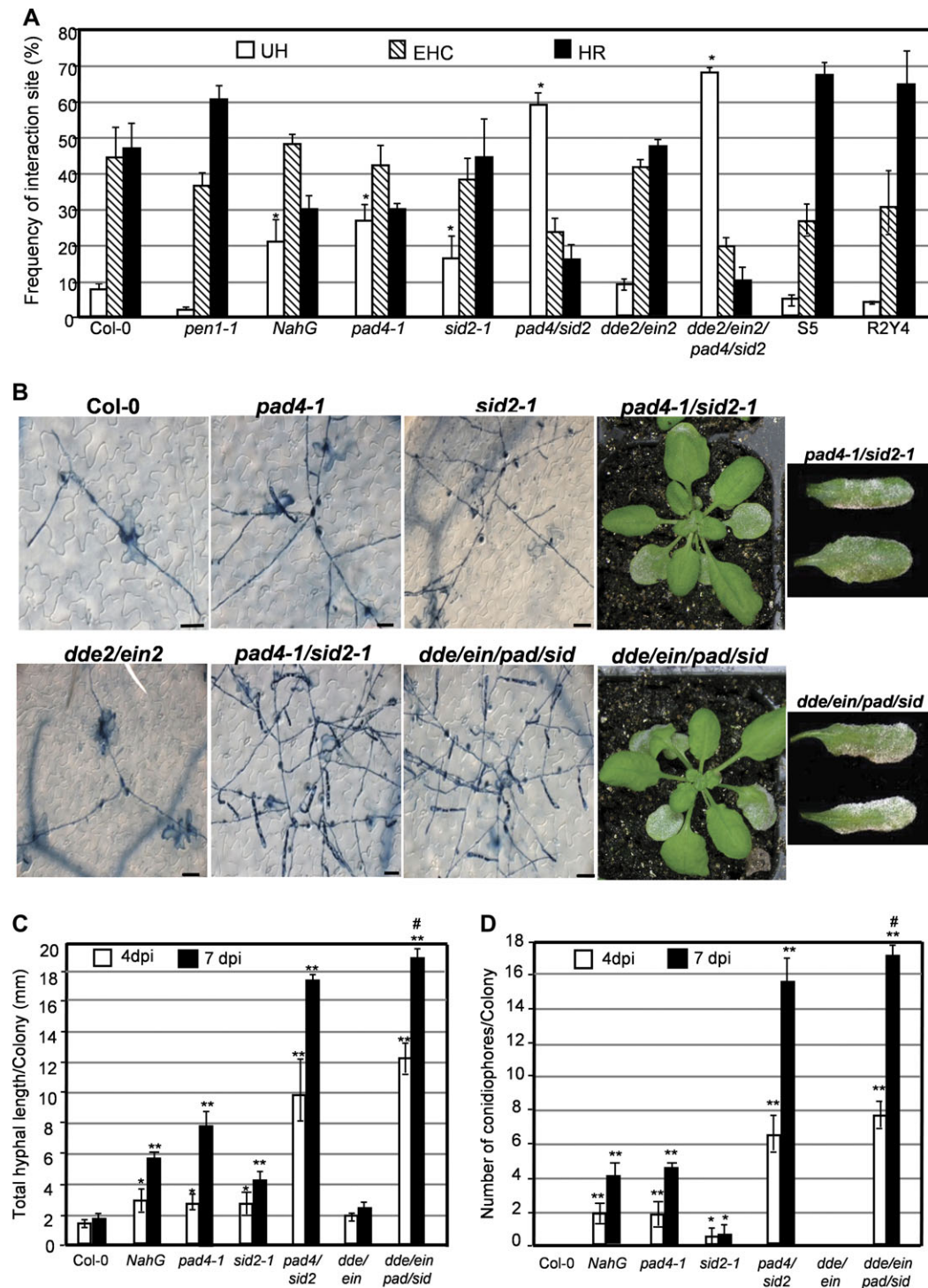


**Fig. 4.** Post-invasion resistance against Gc UMSG1 is controlled by an SA-dependent and SA-independent pathway. (A) Types and frequencies of post-invasion interaction in leaf epidermal cells of the indicated genotypes infected with Gc UMSG1 at 5 dpi. S5 is a Col-0 line transgenic for *RPW8.1* and *RPW8.2* (Xiao *et al.*, 2003); R2Y4 is a Col-0 line transgenic for *RPW8.2-YFP* (Wang *et al.*, 2009). Infected leaves were stained with trypan blue and examined by microscopy. Data are mean  $\pm$  SEM, collected from three independent experiments (for each of which >200 interaction sites/genotype were evaluated).  $\chi^2$ -test is used to test statistical significance for two categorical variables—that is, cells with an unencased haustorium (UH) versus cells with an EHC or undergoing HR, between Col-0 and any other genotype, \* $P$  < 0.05. (B) Representative images showing hyphal growth and sporulation of Gc UMSG1 at 5 dpi (trypan blue-stained leaf sections) or at 10 dpi (whole plant/leaf pictures). Bar, 20  $\mu$ m. (C and D) Total hyphal length (C) and total number of conidiophores (D) per colony of the indicated genotypes infected with Gc UMSG1 at 4 dpi or 7 dpi. Data are mean  $\pm$  SEM (for Student *t*-tests: relative to Col-0, \* $P$  < 0.05, \*\* $P$  < 0.01,  $n$ =3; between *pad4/sid2* and *dde2/ein2/pad4/sid2*, # $P$  < 0.05,  $n$ =3), collected from three independent experiments (for each of which >20 colonies/genotype were evaluated).

*Arabidopsis* but its further development is arrested by post-invasion resistance in *Arabidopsis* controlled by innate immunity components including EDS1.

#### *Encasement of haustorial complex (EHC) and HR cell death contribute to post-invasion resistance in Arabidopsis against Gc UMSG1*

As *Gc* UMSG1 is arrested mainly by post-invasion resistance, it provides an opportunity to examine the possible subcellular responses associated with this layer of non-host resistance using Col-0. To test this idea, plants of Col-0 were first inoculated with *Gc* UCSC1, *Gc* UMSG1, and *Bgh*, and the haustorium development at 2 dpi or 5 dpi was examined by trypan blue staining. Generally there were three types of post-invasion interaction: (i) formation of an unencased, presumably healthy haustorium (i.e. without an EHC); (ii) formation of an encased haustorium (i.e. with an EHC); and (iii) activation of HR cell death. The three representative cell types of *Gc* UMSG1–Col-0 interaction are shown in Fig. 3D. Consistent with *Gc* UCSC1 being a well-adapted pathogen of Col-0, ~95% of interaction sites had formation of unencased haustoria, ~4% of penetrated cells had a haustorium with an EHC, and ~1% of attacked cells underwent HR cell death. In contrast, the frequencies of the (i), (ii), and (iii) interaction types found in Col-0 inoculated with *Gc* UMSG1 were ~8, ~42, and ~49%, respectively. For *Bgh*, ~88% of the rare post-invasion interaction with *Bgh* was accompanied by HR cell death, whereas the remaining ~12% contained a distorted haustorium with a partial EHC (Fig. 3B). These data suggest that both EHC formation and the HR appeared to contribute to post-invasion resistance and the well-adapted powdery mildew isolate *Gc* UCSC1 actively suppresses these defence mechanisms.

#### *Post-invasion resistance against Gc UMSG1 is controlled by both SA-dependent and SA-independent mechanisms*

To determine if the known SA-dependent and/or jasmonic acid (JA)/ethylene (JA/ET)-dependent signalling pathways are involved in post-invasion resistance against *Gc* UMSG1, a panel of *Arabidopsis* mutants (all in the Col-0 background) that are impaired in SA and/or JA/ET signalling were inoculated and the post-invasion interaction was examined by trypan blue staining at 5 dpi. Consistent with the compromised non-host resistance observed in *eds1-2*, it was found that the SA pathway plays an important role in post-invasion resistance, as plants containing *sid2-1* (a mutation impairing SA biosynthesis), *NahG* (encoding salicylate hydrolase), or *pad4-1* (a mutation impairing signalling upstream of SA) supported significantly higher frequencies of unencased haustoria ( $\chi^2$ -test relative to Col-0 for two categorical variables: cells with an unencased haustorium versus cells with an encased haustorium or undergoing HR;  $P < 0.05$ ), with an increase of 9, 14, and 19%, respectively, compared with that of Col-0 (Fig. 4A). A very high rate (~60%) of unencased haustoria was found in the *pad4-1/*

*sid2-1* double mutant, which is a >7-fold increase compared with that of Col-0 and is significantly higher ( $\chi^2$ -test;  $P < 0.05$ ) than that of plants containing *NahG*, *pad4-1*, or *sid2-1* (Fig. 4A). Since *sid2-1* is a mutation in the isochorismate synthase gene involved in SA biosynthesis (Wildermuth et al., 2001), it is likely that loss of PAD4 may contribute to the breakdown of the post-invasion resistance via both the SA-dependent and SA-independent pathways. For the JA/ET pathway-related mutants, it was found that *dde2-2* (JA synthesis) (von Malek et al., 2002), *coi1-1* (JA pathway) (Xie et al., 1998), and *ein2-1* (ET pathway) (Alonso et al., 1999) single mutants, and the *dde2lein2* double mutant (Tsuda et al., 2009) exhibited similar post-invasion interaction patterns to Col-0 (data not shown). However, it was found that the *dde2lein2/pad4/sid2* quadruple mutant consistently supported a higher rate (~68%) of unencased haustoria than the *pad4/sid2* double mutant (Fig. 4A), though the  $\chi^2$  value of 3.33 is just below  $\chi^2_{0.05} = 3.84$ , indicative of no statistical significance.

To examine if increased formation of unencased haustoria in several tested mutants would lead to more hyphal growth and fungal sporulation, seven representative genotypes (Col-0, Col/*NahG*, *pad4-1*, *sid2-1*, *pad4/sid2*, *dde2lein2*, and *dde2lein2/pad4/sid2*) were selected for quantitative assays of the hyphal growth and sporulation by trypan blue staining followed by microscopy at 4 dpi and 7 dpi. It was found that compared with Col-0 plants which supported only limited hyphal growth without formation of any conidiophore, plants of the other six genotypes supported significantly more hyphal growth and weak-to-moderate sporulation (Fig. 4B–D). However, only plants of *pad4-1/sid2-1* and *dde2lein2/pad4/sid2* were found to support profuse fungal growth and sporulation with typical mildew disease symptoms visible to the naked eye at 10 dpi (Fig. 4B). Consistent with the difference observed in the rates of unencased haustoria, *dde2lein2/pad4/sid2* supported significantly (Student *t*-test,  $P < 0.05$ ) more hyphal growth and sporulation measured at 7 dpi when compared with *pad4/sid2* (Fig. 4B–D).

Taken together, the results showed that the invasive growth of *Gc* UMSG1 measured by total hyphal growth and sporulation generally correlated positively with the frequencies of unencased haustoria but negatively with the frequencies of EHC formation and HR. Both SA-dependent (via SID2 and PAD4) and SA-independent (probably via PAD4) pathways, and the JA/ET pathway contribute to post-invasion resistance against *Gc* UMSG1 in *Arabidopsis*.

Experiments were also carried out to examine if post-invasion resistance is altered due to loss of PEN1. It was found that there were actually fewer cells having an unencased haustorium (~2%) but more cells with HR (~60%) in *pen1-1* compared with Col-0 (Fig. 4A). This result was not unexpected given that *pen1-1* exhibited enhanced resistance against *Gc* UCSC1 which was interpreted to be caused by the activation of SA signalling due to loss of PEN1 (Zhang et al., 2007). Therefore, PEN1 did not seem to make a positive contribution to post-invasion resistance against powdery mildew fungi.

*RPW8.2's localization to the extrahaustorial membrane is blocked by the EHC, which may cause excessive HR cell death triggered by Gc UMSG1*

Previous studies showed that *RPW8.2* is specifically targeted to the extrahaustorial membrane (EHM) induced by *Gc* UCSC1, and *RPW8.2*-mediated resistance against this well-adapted pathogen correlates with enhanced EHC formation and HR cell death (Wang *et al.*, 2009). To determine whether *RPW8.2* is also targeted to the EHM induced by *Gc* UMSG1, *Gc* UMSG1-inoculated Col-0 lines either transgenic for *RPW8.1* and *RPW8.2* (S5), or *RPW8.2-YFP* (R2Y4) (all under control of the native promoters) were examined at 5 dpi. Compared with Col-0, plants expressing *RPW8.1* and/or *RPW8.2* had lower frequencies (<5%) of cells containing an unencased haustorium and most of the invaded cells (~66%) underwent cell death (Fig. 4A). Because all tested *Arabidopsis* accessions (see Materials and methods) including those lacking *RPW8.1* and *RPW8.2* showed robust post-invasion resistance to *Gc* UMSG1 (data not shown), it was apparent that a very high HR cell death rate caused by *RPW8.2* may be costly and unnecessary. To understand why *RPW8.2* is more potent in triggering HR in cells invaded by *Gc* UMSG1, the spatiotemporal *RPW8.2:YFP* expression in leaves of R2Y4 plants inoculated with *Gc* UMSG1 was monitored. Surprisingly, *RPW8.2:YFP* was rarely (<5%) found in the EHM. Instead, it was often found in punctate spots accumulated in the periphery of the EHC or in mobile vesicles probably in the trafficking pathway (Fig. 5A, B). These cells showed rapid induced whole-cell H<sub>2</sub>O<sub>2</sub> accumulation as early as 20 hpi and soon (~30 hpi) underwent HR cell death as shown by trypan blue staining (Fig. 5H, I). This reaction phenotype is reminiscent of what is observed in S5/*pmr4-1* plants (Wang *et al.*, 2009) in which the EHC is perturbed by loss of *PMR4/GSL5*, the callose synthase responsible for synthesis of the callose deposited to the EHC (Jacobs *et al.*, 2003; Nishimura *et al.*, 2003). Thus, it appeared that rapid EHC formation in response to the haustorial invasion from *Gc* UMSG1 may physically block the targeting of *RPW8.2* vesicles to the EHM. This may result in accumulation of *RPW8.2* vesicles outside of the EHC, leading to *RPW8.2*-triggered H<sub>2</sub>O<sub>2</sub> production and accumulation in the cytoplasm, and subsequent HR cell death. To see if reduced EHC formation would allow increased localization of *RPW8.2* to the EHM, the *RPW8.2-YFP* construct was introduced into *pad4-1/sid2-1* in which the frequency of unencased haustoria was significantly increased (Fig. 4A). Using laser scanning confocal microscopy, frequent EHM localization of *RPW8.2:YFP* was indeed observed in ~60% of *pad4-1/sid2-1* cells invaded by haustoria of *Gc* UMSG1 (Fig. 5C), similar to what is seen in cells of R2Y4 infected by *Gc* UCSC1 (Wang *et al.*, 2009). In the remaining ~40% of invaded cells several intermediate localization patterns were observed, with weaker *RPW8.2:YFP* signal found in part of the EHM where the callose in the EHC was detectable by sirofluoro (Fig. 5D–F) or with no obvious accumulation of

*RPW8.2:YFP* at the EHM of deformed haustoria contained by a thick EHC (Fig. 5G). Not surprisingly, *pad4-1/sid2-1* plants transgenic for *RPW8.2-YFP* showed frequencies of EHC formation and HR not significantly different from that of *pad4-1/sid2-1* alone (data not shown), which is consistent with previous findings that *RPW8.2*'s defence activity is SA and/or PAD4 dependent (Xiao *et al.*, 2003, 2005).

## Discussion

*Arabidopsis*–powdery mildew interaction has been successfully used as the model pathosystem to study both host and non-host resistance mechanisms at the molecular level over the past 15 years (Adam and Somerville, 1996; Reuber *et al.*, 1998; Collins *et al.*, 2003; Nishimura *et al.*, 2003; Lipka *et al.*, 2005; Stein *et al.*, 2006). Most studies on this topic were conducted by using four powdery mildews: *Bgh* and *E. pisi*, two non-adapted isolates, and *Gc* UCSC1 and *G. orontii*, two well-adapted isolates. In this study, a sow thistle powdery mildew isolate *Gc* UMSG1 was identified as a non-host pathogen of *Arabidopsis* with some limited, early-stage adaptation: *Gc* UMSG1 has largely overcome penetration resistance but its haustorium development and/or function is invariably terminated by post-invasion resistance in all tested *Arabidopsis* accessions. This limited adaptation on *Arabidopsis* implies that *Gc* UMSG1 may be able to survive and reproduce on close relatives of *Arabidopsis*, hence the limited adaption on *Arabidopsis*. It should be pointed out that many powdery mildew isolates with distinct adaptation on dicots are classified as *G. cichoracearum* (Garibaldi *et al.*, 2008; Gevens *et al.*, 2009; Troisi *et al.*, 2010). This situation is somehow reminiscent of formae speciales formation of *B. graminis* on grasses (Wyand and Brown, 2003). Thus, characterization of *G. cichoracearum* formae speciales probably requires higher resolution phylogenetic analyses and comparative host-range determination. The resultant high frequency (~43%) of EHC induction by *Gc* UMSG1 in wild-type *Arabidopsis* Col-0 (Fig. 4A) makes *Gc* UMSG1 distinct from *Bgh*. Therefore, *Gc* UMSG1 can be a useful, complementary tool to investigate post-invasion resistance which probably represents the last lines of non-host immunity against powdery mildew pathogens in *Arabidopsis*.

The present data showed that both the formation of the callosic EHC and HR cell death are associated with post-invasion resistance against *Gc* UMSG1 (Fig. 4). Similar haustorial encasement structures have long been recognized to be associated with host defence in monocot and dicot plants when challenged by non-adapted or adapted fungal and oomycete pathogens (Ehrlich and Ehrlich, 1963; Perumalla and Heath, 1989; Skalamera and Heath, 1995; Starknau and Mendgen, 1995; Heath *et al.*, 1996; Silva *et al.*, 1999; Soyly and Soyly, 2003; Soyly *et al.*, 2004). Thus, EHC formation may be a conserved cellular defence mechanism against haustorial invasion in plants.

Earlier studies suggested that papillae contain callose (β-1,3-glucan), phenolic compounds, lignin, and reactive

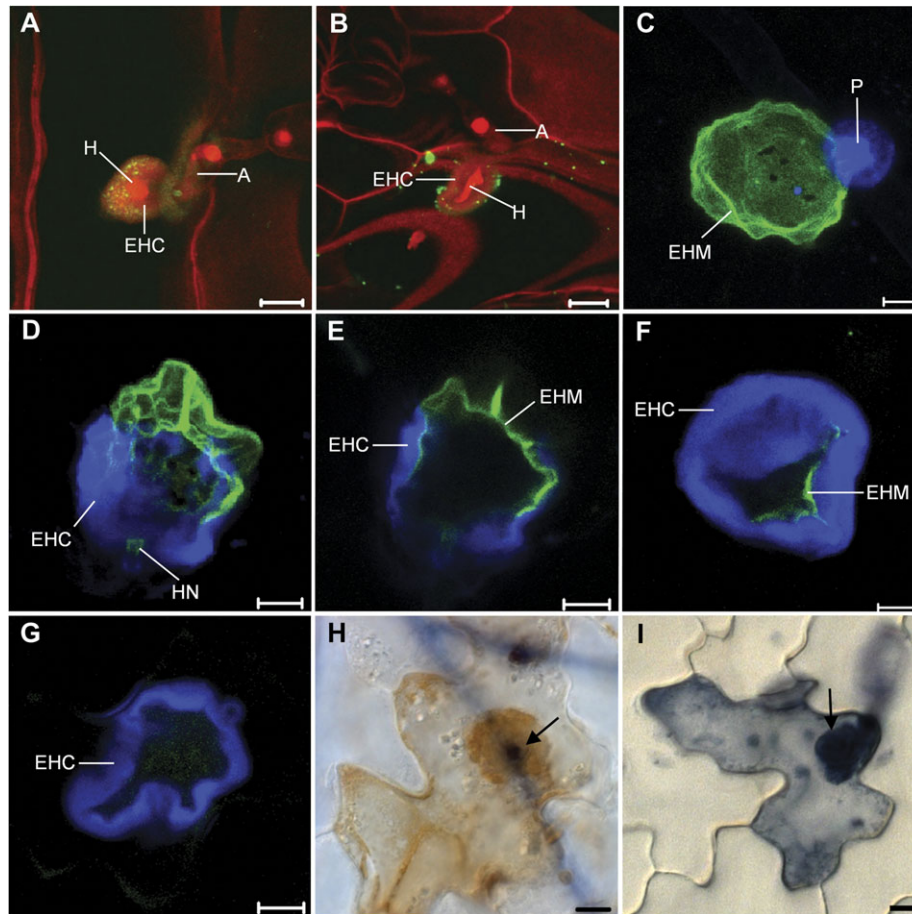


**Fig. 5.** Targeting of RPW8.2:YFP to the extrahaustorial membrane (EHM) may be blocked by the encasement of the haustorial complex (EHC). (A and B) Col-0 expressing *RPW8.2:YFP* was inoculated with *Gc UMSG1* and the infected leaves were subjected to propidium iodide (PI) staining followed by confocal microscopy at 24 hpi. RPW8.2:YFP was detected in punctate spots on or peripheral to the weakly PI-positive EHC (A and B) or elsewhere probably in the trafficking pathway (B). (C–G) A *pad4-1/sid2-1* double mutant line transgenic for *RPW8.2:YFP* was inoculated with *Gc UMSG1* and the infected leaves were subject to confocal microscopy at 24 hpi. Targeting of RPW8.2:YFP to the EHM appeared to be normal in the absence of the EHC (C), or partially compromised due to formation of an incomplete EHC (D–F). In some cases, RPW8.2:YFP signal was undetectable in the EHM or cytoplasm in cells having a haustorium constrained by a complete EHC (G). Pictures in A to D were Z-stack projections of 20–25 confocal images, and images in E to G were from single optical sections. The EHC was highlighted by callose stained by sirofluoro (Meyer *et al.*, 2009) and fungal structures and host cell wall and membrane were stained red by PI (Wang *et al.*, 2009). H, haustorium; A, appressorium; P, papilla; HN, haustorial neck. Bars, 10 µm (A, B), 5 µm (C–G). (H–I) Representative images showing accumulation of  $H_2O_2$  (indicated by brownish colour) detected by 3,3'-diaminobenzidine staining (H), or cell death (indicated by blue colour) detected by trypan blue staining (I) in a *pad4/sid2* lines expressing *RPW8.2:YFP* infected with *Gc UMSG1* at 4 dpi. Arrows indicate penetration sites. Bars, 20 µm.

oxygen species (Aist, 1976; Israel *et al.*, 1980; Thordal-Christensen *et al.*, 1997). However, the physical and chemical nature of the EHC is less characterized (Meyer *et al.*, 2009; Wang *et al.*, 2009) and little is known about the cellular machinery engaged in EHC formation. Donofrio and Delaney (2001) showed that induction of the EHC in *Arabidopsis* mesophyll cells by an adapted *Hyaloperonospora arabidopsidis* isolate is compromised by expression of *NahG* or loss of *NIM1* (*NPRI*), a master regulator of defence signalling downstream of SA. This observation suggested a role for the SA-dependent signalling in EHC formation. From the data in Fig. 4, EHC formation induced by *Gc UMSG1* did not seem to be significantly affected in *NahG*-expressing plants, or in *pad4-1* or *sid2-1* single

mutants, but those plants supported increased (9–19%) frequencies of unencased haustoria, resulting in more hyphal growth and low levels of sporulation. Thus, this partial breakdown of post-invasion resistance seemed to be associated with lower frequencies of HR cells compared with that of wild-type Col-0. However, it should be pointed out that many cells undergoing HR contain a haustorium with an EHC but were scored as the HR type in the present experiments. The classification of EHC formation and HR into two distinct interaction types was an expedient simplification to reflect EHC formation as a subcellular defence response. In reality, an invaded cell having EHC at one time point could be scored as having HR at a slightly later time point. Hence, while the frequency of unencased

haustoria reflects the well-being of the invading fungus, EHC formation together with HR reflects host defence response. The *pad4-1/sid2-1* double mutant became almost fully susceptible to *Gc* UMSG1, suggesting that either PAD4 and SID2 can compensate for each other's function in post-invasion resistance, similar to their contribution to AvrRpt2-RPS2-triggered race-specific host resistance (Tsuda *et al.*, 2009), or both SA-dependent (SID2 and PAD4) and SA-independent (PAD4) defence mechanisms are involved in post-invasion resistance. This result is consistent with earlier observations that PAD4 and its homologous partner EDS1 regulate both SA-dependent and SA-independent defence signalling (Bartsch *et al.*, 2006; Venugopal *et al.*, 2009). The contribution of the JA/ET pathway to post-invasion resistance against powdery mildew is rather subtle, because a statistically significant difference in disease phenotypes between single or double JA/ET pathway mutants and Col-0 inoculated with *Gc* UMSG1 or *Gc* UCSC1 was not detected (data not shown; Xiao *et al.*, 2005). However, more fungal growth of *Gc* UMSG1 in *dde2/ein2/pad4/sid2* than in *pad4/sid2* was observed (Fig. 4B–D), although no significant difference in the growth of *Gc* UCSC1 was seen between these two genotypes (data not shown). Zimmerli and co-authors found that non-adapted (*Bgh*) but not host-adapted powdery mildew (*Gc* UCSC1) induced expression of the defence genes controlled by the JA/ET pathway (Zimmerli *et al.*, 2004). Thus, it seems likely that the JA/ET pathway has a minor contribution to post-invasion resistance against non-adapted/poorly adapted powdery mildew, which can be more readily detectable in plants whose immunity system is already severely compromised. The present results also support the speculation that well-adapted powdery mildew suppresses the JA/ET pathway (Zimmerli *et al.*, 2004) and are compatible with the model that there exist synergistic relationships among different defence signalling pathways in basal resistance (Tsuda *et al.*, 2009).

In a previous study, it was found that both EHC formation and the HR correlated with RPW8.2-mediated host resistance against the adapted powdery mildew isolate *Gc* UCSC1 (Wang *et al.*, 2009). Thus, EHC formation and the HR may be the common cellular defence mechanisms against haustorial invasion in the post-invasion stage regardless of whether it is from non-adapted or well-adapted pathogens. Combined with earlier studies, the present work supports a co-evolutionary scenario for the interaction between haustorium-forming pathogens such as powdery mildew and their target plants as follows. For non-adapted powdery mildews, their entry into the host cell is stopped by penetration resistance manifested as the formation of papillae (Thordal-Christensen, 2003). When penetration resistance is gradually broken down, haustorium development and/or function is terminated by post-invasion resistance manifested as EHC formation and the HR. Adapted powdery mildew pathogens must have evolved the ability to suppresses EHC formation and the HR in order to sustain their haustorium function; in response, host plants have then evolved RPW8.2 or RPW8.2-like proteins

to counter this suppression, thereby enhancing post-invasion resistance.

The present examination of RPW8.2:YFP localization in *Gc* UMSG1-invaded cells (Fig. 5) provided unexpected mechanistic insight into how RPW8.2 might cause excessive HR cell death. In cases where an EHC was rapidly formed, RPW8.2's targeting to the EHM was then hindered, resulting in accumulation of RPW8.2 peripheral to the EHC or in the trafficking pathway. Inappropriately localized RPW8.2 may trigger whole-cell H<sub>2</sub>O<sub>2</sub> accumulation, leading to HR cell death. This speculation is consistent with earlier observations that RPW8.2 overexpression from its native promoter triggers HR-like cell death (Xiao *et al.*, 2003) and that genetic perturbation of the actin cytoskeleton by overexpression of *ADF6* results in RPW8.2 accumulation in punctate spots and subsequent cell death (Wang *et al.*, 2009). This finding also raised interesting questions as to whether the focal accumulation of callose and other components in the EHC and RPW8.2 or RPW8.2-like proteins in the EHM is conducted via the same or two separate polarized trafficking pathways and how these events are spatiotemporally orchestrated. A previous study showed that RPW8.2's EHM localization does not seem to be affected in the *pen1-1* mutant (Wang *et al.*, 2009), whereas the assembly of the callosic papilla is delayed due to loss of PEN1-defined exocytosis (Assaad *et al.*, 2004). Given the blockage of RPW8.2:YFP outside of the EHC induced by *Gc* UMSG1, it is likely that targeting of RPW8.2 to the EHM may occur at the same or a later stage as for the EHC formation induced by *Gc* UMSG1 via a PEN1-independent/redundant exocytosis pathway.

Because (i) the EHC appears to have a similar physical structure to papillae and may actually originate from expansion of the papilla via rim growth (Meyer *et al.*, 2009), which is also supported by the present observations (Fig. 5C–E) and (ii) GFP:PEN1 is selectively incorporated into the EHC, even though callose deposition to the EHC is not apparently affected in *pen1-1* (Meyer *et al.*, 2009), one may wonder if exocytosis dependent on PEN1 and/or its close homologue SYP122 contributes to deposition of other materials in the EHC. The present result showed that EHC formation induced by *Gc* UMSG1 was slightly reduced (by ~8%) in *pen1-1*, but there was an increase in the frequency of HR (by ~14%) in *pen1-1* when compared with that of Col-0 (Fig. 4A). It remains unclear whether EHC formation is dependent on PEN1's function. Future studies using *Gc* UMSG1 as an EHC-inducible non-adapted pathogen of *Arabidopsis* and a *pen1/syp122* double mutant in a genetic background where HR cell death is suppressed may be able to determine if these two syntaxins contribute to EHC formation as a general cellular defence response in plants.

## Acknowledgements

We are grateful to Roger Wise and Gregory Fuerst for providing barley seeds and the *B. graminis* f. sp. *horde* isolate, Shauna Somerville for the *G. cichoracearum* UCSC1 isolate, Hans Thordal-Christensen for *pen1-1* seeds, Lori

Urban for technical support, Grace Yang for advice on statistical analyses, and Zhanao Deng and the Xiao lab members for critical reading of this manuscript. Funding for this study was provided by a scholarship from the Ministry of Education of the People's Republic of China and a grant from the National Science Foundation of China (31071772) to YW and JF, and by the National Science Foundation Grant IOS-0842877 to SX and MCB-0918908 to FK.

## References

- Aarts N, Metz M, Holub E, Staskawicz BJ, Daniels MJ, Parker JE.** 1998. Different requirements for *EDS1* and *NDR1* by disease resistance genes define at least two *R* gene-mediated signaling pathways in Arabidopsis. *Proceedings of the National Academy of Sciences, USA* **95**, 10306–10311.
- Adam L, Ellwood S, Wilson I, Saenz G, Xiao S, Oliver RP, Turner JG, Somerville S.** 1999. Comparison of *Erysiphe cichoracearum* and *E. cruciferarum* and a survey of 360 *Arabidopsis thaliana* accessions for resistance to these two powdery mildew pathogens. *Molecular Plant-Microbe Interactions* **12**, 1031–1043.
- Adam L, Somerville SC.** 1996. Genetic characterization of five powdery mildew disease resistance loci in *Arabidopsis thaliana*. *The Plant Journal* **9**, 341–356.
- Aist JR.** 1976. Papillae and related wound plugs of plant-cells. *Annual Review of Phytopathology* **14**, 145–163.
- Alonso JM, Hirayama T, Roman G, Nourizadeh S, Ecker JR.** 1999. EIN2, a bifunctional transducer of ethylene and stress responses in Arabidopsis. *Science* **284**, 2148–2152.
- Assaad FF, Qiu JL, Youngs H, et al.** 2004. The PEN1 syntaxin defines a novel cellular compartment upon fungal attack and is required for the timely assembly of papillae. *Molecular Biology of the Cell* **15**, 5118–5129.
- Bartsch M, Gobbato E, Bednarek P, Debey S, Schultze JL, Bautor J, Parker JE.** 2006. Salicylic acid-independent ENHANCED DISEASE SUSCEPTIBILITY1 signaling in Arabidopsis immunity and cell death is regulated by the monooxygenase FMO1 and the nudix hydrolase NUDT7. *The Plant Cell* **18**, 1038–1051.
- Bednarek P, Pislewska-Bednarek M, Svatos A, et al.** 2009. A glucosinolate metabolism pathway in living plant cells mediates broad-spectrum antifungal defense. *Science* **323**, 101–106.
- Chisholm ST, Coaker G, Day B, Staskawicz BJ.** 2006. Host-microbe interactions: shaping the evolution of the plant immune response. *Cell* **124**, 803–814.
- Clay NK, Adio AM, Denoux C, Jander G, Ausubel FM.** 2009. Glucosinolate metabolites required for an Arabidopsis innate immune response. *Science* **323**, 95–101.
- Collins NC, Thordal-Christensen H, Lipka V, et al.** 2003. SNARE-protein-mediated disease resistance at the plant cell wall. *Nature* **425**, 973–977.
- Dangl JL, Jones JD.** 2001. Plant pathogens and integrated defence responses to infection. *Nature* **411**, 826–833.
- Donofrio NM, Delaney TP.** 2001. Abnormal callose response phenotype and hypersusceptibility to *Peronospora parasitica* in defence-compromised arabidopsis *nim1-1* and salicylate hydroxylase-expressing plants. *Molecular Plant-Microbe Interactions* **14**, 439–450.
- Ehrlich HG, Ehrlich MA.** 1963. Electron microscopy of sheath surrounding haustorium of *Erysiphe graminis*. *Phytopathology* **53**, 1378–1380.
- Falk A, Feys BJ, Frost LN, Jones JD, Daniels MJ, Parker JE.** 1999. *EDS1*, an essential component of *R* gene-mediated disease resistance in Arabidopsis has homology to eukaryotic lipases. *Proceedings of the National Academy of Sciences, USA* **96**, 3292–3297.
- Garibaldi A, Bertetti D, Frati S, Minuto A, Gullino ML.** 2008. Powdery mildew caused by *Golovinomyces cichoracearum* on Paris daisy (*Argyranthemum frutescens*) in Italy. *Plant Disease* **92**, 1135–1135.
- Gevens AJ, Maia G, Jordan SA.** 2009. First report of powdery mildew caused by *Golovinomyces cichoracearum* on *Crotalaria juncea* ('Tropic Sun' Sunn hemp). *Plant Disease* **93**, 427–427.
- Hadwiger LA, Culley DE.** 1993. Nonhost resistance genes and race-specific resistance. *Trends in Microbiology* **1**, 136–141.
- Halterman D, Zhou F, Wei F, Wise RP, Schulze-Lefert P.** 2001. The MLA6 coiled-coil, NBS-LRR protein confers AvrMla6-dependent resistance specificity to *Blumeria graminis* f. sp. *hordei* in barley and wheat. *The Plant Journal* **25**, 335–348.
- Heath MC, Xu HX, Eilam T.** 1996. Nuclear behavior of the cowpea rust fungus during the early stages of basidiospore- or urediospore-derived growth in resistant or susceptible cowpea cultivars. *Phytopathology* **86**, 1057–1065.
- Israel HW, Wilson RG, Aist JR, Kunoh H.** 1980. Cell-wall appositions and plant-disease resistance—acoustic microscopy of papillae that block fungal ingress. *Proceedings of the National Academy of Sciences, USA* **77**, 2046–2049.
- Jacobs AK, Lipka V, Burton RA, Panstruga R, Strizhov N, Schulze-Lefert P, Fincher GB.** 2003. An Arabidopsis callose aynthase, GSL5, is required for wound and papillary callose formation. *The Plant Cell* **15**, 2503–2513.
- Jirage D, Tootle TL, Reuber TL, Frost LN, Feys BJ, Parker JE, Ausubel FM, Glazebrook J.** 1999. Arabidopsis thaliana PAD4 encodes a lipase-like gene that is important for salicylic acid signaling. *Proceedings of the National Academy of Sciences, USA* **96**, 13583–13588.
- Jones JD, Dangl JL.** 2006. The plant immune system. *Nature* **444**, 323–329.
- Kwon C, Neu C, Pajonk S, et al.** 2008. Co-option of a default secretory pathway for plant immune responses. *Nature* **451**, 835–840.
- Lipka V, Dittgen J, Bednarek P, et al.** 2005. Pre- and postinvasion defenses both contribute to nonhost resistance in Arabidopsis. *Science* **310**, 1180–1183.
- Mellersh DG, Heath MC.** 2003. An investigation into the involvement of defense signaling pathways in components of the nonhost resistance of Arabidopsis thaliana to rust fungi also reveals a model system for studying rust fungal compatibility. *Molecular Plant-Microbe Interactions* **16**, 398–404.
- Meyer D, Pajonk S, Micali C, O'Connell R, Schulze-Lefert P.** 2009. Extracellular transport and integration of plant secretory proteins

into pathogen-induced cell wall compartments. *The Plant Journal* **57**, 986–999.

**Nishimura MT, Stein M, Hou BH, Vogel JP, Edwards H, Somerville SC.** 2003. Loss of a callose synthase results in salicylic acid-dependent disease resistance. *Science* **301**, 969–972.

**Nurnberger T, Brunner F, Kemmerling B, Piater L.** 2004. Innate immunity in plants and animals: striking similarities and obvious differences. *Immunological Reviews* **198**, 249–266.

**Orgil U, Araki H, Tangchaiburana S, Xiao S.** 2007. Intraspecific genetic variations, fitness cost and benefit of *RPW8*, a disease resistance locus in *Arabidopsis thaliana*. *Genetics* **176**, 2317–2333.

**Parker JE, Holub EB, Frost LN, Falk A, Gunn ND, Daniels MJ.** 1996. Characterization of *eds1*, a mutation in *Arabidopsis* suppressing resistance to *Peronospora parasitica* specified by several different RPP genes. *The Plant Cell* **8**, 2033–2046.

**Perumalla CJ, Heath MC.** 1989. Effect of callose inhibition on haustorium formation by the cowpea rust fungus in the non-host, bean plant. *Physiological and Molecular Plant Pathology* **35**, 375–382.

**Reuber TL, Plotnikova JM, Dewdney J, Rogers EE, Wood W, Ausubel FM.** 1998. Correlation of defense gene induction defects with powdery mildew susceptibility in *Arabidopsis* enhanced disease susceptibility mutants. *The Plant Journal* **16**, 473–485.

**Silva MC, Nicole M, Rijo L, Geiger JP, Rodrigues CJ.** 1999. Cytochemical aspects of the plant–rust fungus interface during the compatible interaction *Coffea arabica* (cv. Caturra) *Hemileia vastatrix* (Race III). *International Journal of Plant Sciences* **160**, 79–91.

**Skalamera D, Heath MC.** 1995. Changes in the plant endomembrane system associated with callose synthesis during the interaction between cowpea (*Vigna unguiculata*) and the cowpea rust fungus (*Uromyces vignae*). *Canadian Journal of Botany-Revue Canadienne De Botanique* **73**, 1731–1738.

**Soylu EM, Soylu S.** 2003. Light and electron microscopy of the compatible interaction between *Arabidopsis* and the downy mildew pathogen *Peronospora parasitica*. *Journal of Phytopathology-Phytopathologische Zeitschrift* **151**, 300–306.

**Soylu EM, Soylu S, Mansfield JW.** 2004. Ultrastructural characterisation of pathogen development and host responses during compatible and incompatible interactions between *Arabidopsis thaliana* and *Peronospora parasitica*. *Physiological and Molecular Plant Pathology* **65**, 67–78.

**Starknau M, Mendgen K.** 1995. Sequential deposition of plant glycoproteins and polysaccharides at the host–parasite interface of *Uromyces vignae* and *Vigna sinensis*—evidence for endocytosis and secretion. *Protoplasma* **186**, 1–11.

**Stein M, Dittgen J, Sanchez-Rodriguez C, Hou BH, Molina A, Schulze-Lefert P, Lipka V, Somerville S.** 2006. *Arabidopsis* PEN3/PDR8, an ATP binding cassette transporter, contributes to nonhost resistance to inappropriate pathogens that enter by direct penetration. *The Plant Cell* **18**, 731–746.

**Tamura K, Dudley J, Nei M, Kumar S.** 2007. MEGA4: Molecular Evolutionary Genetics Analysis (MEGA) software version 4.0. *Molecular Biology and Evolution* **24**, 1596–1599.

**Thordal-Christensen H.** 2003. Fresh insights into processes of nonhost resistance. *Current Opinion in Plant Biology* **6**, 351–357.

**Thordal-Christensen H, Zhang ZG, Wei YD, Collinge DB.** 1997. Subcellular localization of H<sub>2</sub>O<sub>2</sub> in plants. H<sub>2</sub>O<sub>2</sub> accumulation in papillae and hypersensitive response during the barley–powdery mildew interaction. *The Plant Journal* **11**, 1187–1194.

**Troisi M, Bertetti D, Garibaldi A, Gullino ML.** 2010. First report of powdery mildew caused by *Golovinomyces cichoracearum* on *Gerbera* (*Gerbera jamesonii*) in Italy. *Plant Disease* **94**, 130–130.

**Tsuda K, Sato M, Stoddard T, Glazebrook J, Katagiri F.** 2009. Network properties of robust immunity in plants. *PLoS Genetics* **5**, e1000772.

**Venugopal SC, Jeong RD, Mandal MK, et al.** 2009. Enhanced disease susceptibility 1 and salicylic acid act redundantly to regulate resistance gene-mediated signaling. *PLoS Genetics* **5**, e1000545.

**von Malek B, van der Graaff E, Schneitz K, Keller B.** 2002. The *Arabidopsis* male-sterile mutant *dde2-2* is defective in the ALLENE OXIDE SYNTHASE gene encoding one of the key enzymes of the jasmonic acid biosynthesis pathway. *Planta* **216**, 187–192.

**Wang W, Wen Y, Berkey R, Xiao S.** 2009. Specific targeting of the *Arabidopsis* resistance protein RPW8.2 to the interfacial membrane encasing the fungal haustorium renders broad-spectrum resistance to powdery mildew. *The Plant Cell* **21**, 2898–2913.

**Wildermuth MC, Dewdney J, Wu G, Ausubel FM.** 2001. Isochorismate synthase is required to synthesize salicylic acid for plant defence. *Nature* **414**, 562–565.

**Wyand RA, Brown JK.** 2003. Genetic and forma specialis diversity in *Blumeria graminis* of cereals and its implications for host–pathogen co-evolution. *Molecular Plant Pathology* **4**, 187–198.

**Xiao S, Brown S, Patrick E, Brearley C, Turner JG.** 2003. Enhanced transcription of the *Arabidopsis* disease resistance genes RPW8.1 and RPW8.2 via a salicylic acid-dependent amplification circuit is required for hypersensitive cell death. *The Plant Cell* **15**, 33–45.

**Xiao S, Calis O, Patrick E, Zhang G, Charoenwattana P, Muskett P, Parker JE, Turner JG.** 2005. The atypical resistance gene, RPW8, recruits components of basal defence for powdery mildew resistance in *Arabidopsis*. *The Plant Journal* **42**, 95–110.

**Xiao S, Ellwood S, Calis O, Patrick E, Li T, Coleman M, Turner JG.** 2001. Broad-spectrum mildew resistance in *Arabidopsis thaliana* mediated by RPW8. *Science* **291**, 118–120.

**Xie DX, Feys BF, James S, Nieto-Rostro M, Turner JG.** 1998. COI1: an *Arabidopsis* gene required for jasmonate-regulated defense and fertility. *Science* **280**, 1091–1094.

**Yun BW, Atkinson HA, Gaborit C, Greenland A, Read ND, Pallas JA, Loake GJ.** 2003. Loss of actin cytoskeletal function and EDS1 activity, in combination, severely compromises non-host resistance in *Arabidopsis* against wheat powdery mildew. *The Plant Journal* **34**, 768–777.

**Zhang Z, Feechan A, Pedersen C, Newman MA, Qiu JL, Olesen KL, Thordal-Christensen H.** 2007. A SNARE-protein has opposing functions in penetration resistance and defence signalling pathways. *The Plant Journal* **49**, 302–312.

**Zimmerli L, Stein M, Lipka V, Schulze-Lefert P, Somerville S.** 2004. Host and non-host pathogens elicit different jasmonate/ethylene responses in *Arabidopsis*. *The Plant Journal* **40**, 633–646.